Analytical and Bioanalytical Chemistry (2022) 414:2029–2040
https://doi.org/10.1007/s00216-021-03849-9

PAPER IN FOREFRONT

Signal-on/signal-off bead-based assays for the multiplexed monitoring of base excision repair activities by flow cytometry

Guillaume Gines[1] · Charlotte Brusa[2] · Christine Saint-Pierre[2] · Didier Gasparutto[2]

Received: 22 October 2021 / Revised: 3 December 2021 / Accepted: 13 December 2021 / Published online: 23 January 2022

Abstract

As the support of all living kingdoms' genetic information, the integrity of the DNA biomolecule must be preserved. To that goal, cells have evolved specific DNA repair pathways to thwart a large diversity of chemical substances and radiations that alter the DNA structure and lead to the development of pathologies such as cancers or neurodegenerative diseases. When dysregulated, activity rates of various actors of DNA repair can play a key role in carcinogenesis as well as in drugs resistance or hypersensitivity mechanisms. For the last 10 years, new complementary treatments have aimed at targeting specific enzymes responsible for such resistances. It is therefore crucial for biomedical research and clinical diagnosis to develop fast and sensitive tools able to measure the activity rate of DNA repair enzymes. In this work, a new assay for measuring enzymatic activities using microbeacons (μBs) is expounded. μB refers to microsphere functionalized by hairpin-shaped nucleic acid probes containing a single site-specific lesion in the stem and modified with chromophores. Following the processing of the lesion by the targeted protein, μB is cleaved and either lights off (signal-off strategy) or on (signal-on), depending on the use of fluorescent or profluorescent probes, respectively. After an optimization phase of the assay, we reported the combined analysis of restriction enzyme, AP-endonuclease, and DNA *N*-glycosylase by real-time monitoring followed by a flow cytometry measurement. As proofs of concept, we demonstrated the potential of the biosensor for highlighting DNA repair inhibitors and discriminating cell lines from their enzymatic activities.

Keywords Base excision repair · Bead-based assay · Flow cytometry · Real-time monitoring · Microbeacon

Introduction

Despite its crucial biological roles in the development, functioning, maintenance of genetic integrity, and reproduction of organisms, DNA remains a sensitive molecule. It presents a non-negligible reactivity towards endogenous (reactive oxygen species, polyunsaturated fatty acids, etc.) and exogenous species (UV radiations, chemicals, etc.), causing alterations that may lead to the development of pathologies such as cancers, neurodegenerative, or genetic disorders [1–3]. Fortunately, cells possess specific DNA repair mechanisms to thwart a large diversity of DNA damages [4, 5]. DNA repair effectors may also play a key role in carcinogenesis as well as in drug resistance or hypersensitivity mechanisms. In the first case, dysfunctions in a single or several repair pathways may cause the persistence of lesions that might be converted into mutations at the onset of carcinogenesis [6–9]. In the second case, overexpression of DNA repair enzymes may counteract anticancer treatments by removing damages caused by chemo- or radio-therapeutic agents [10, 11]. For the last decades, new complementary treatments have aimed to target DNA repair enzymes responsible for such resistances [12–14].

Base excision repair (BER) is a crucial DNA repair pathway responsible for restoring a large panel of DNA lesions [7, 15, 16]. These include oxidized, alkylated or hydrolyzed nitrogenous bases, and abasic (AP) sites. The biochemical mechanism of BER can be segmented into sequential steps involving different enzymes that process the lesion and give way to the next intermediate according to the simplified model of "passing the baton." Firstly, the lesion is recognized by a specific DNA *N*-glycosylase that hydrolyzes the *N*-glycosidic bond, releasing an AP site. Then, an

✉ Guillaume Gines
guillaume.gines@espci.fr

[1] Laboratoire Gulliver, CNRS, ESPCI Paris, PSL Research University, 10 rue Vauquelin, 75005 Paris, France

[2] University Grenoble Alpes, CEA, CNRS, IRIG, SyMMES-UMR5819, 38000 Grenoble, France

AP-endonuclease incises the phosphodiester bond directly in 5' of the AP site. In the predominant short-path repair, the resulting 5'-deoxyribophosphate is removed by an AP-lyase and the gap is filled by a polymerase (e.g., pol β). Finally, strand continuity is restored by a DNA ligase. BER is recognized as a central metabolic pathway involved obviously in DNA repair, but also in the innate and acquired immunity as well as in epigenetic regulation of genes expression. Additionally, various disorders such as hyper IgM syndrome type V (HIGM5), ataxia with oculomotor apraxia type I (AOA1), or MUTYH-associated polyposis (MAP) are caused by a deficiency in BER [17–20].

It remains paramount in biomedical research and medical diagnosis to develop fast and sensitive tools able to measure base excision repair capacities of cells, tissues, or individuals [21, 22]. This would be suitable to develop targeted anticancer treatments, with high efficacy and limited secondary effects, or to establish a screening platform for potential DNA repair inhibitors [13, 23]. Current methods use fluorescent or radioactive probes containing specific DNA lesions to detect the cleavage occurring by the joined action of a monofunctional glycosylase and AP-endonuclease or by a bifunctional glycosylase. DNA fragments are classically analyzed by polyacrylamide gel electrophoresis, ill-adapted to multiplexing and high-throughput screening [24–28]. To circumvent the limitations of separative techniques (low sensitivity, lengthy protocols), numerous studies have reported the use of molecular beacons to monitor enzymatic cleavage [29, 30]. Initially developed to detect nucleic acids, molecular beacons denote hairpin-shaped structure (a double-stranded stem connected by a single-stranded nucleic acid loop) whose two extremities are labeled with a fluorophore and a quencher. For sensing BER activities, the targeted DNA lesion is selectively introduced in the stem. In the closed, initial conformation, the two chromophores are brought in proximity, quenching photon emission. When the lesion is processed, the resulting cleavage induces the disruption of the hairpin structure, which results in the separation of the two dyes and restores fluorescence emission. These original probes are a powerful analytical tool for sensitive and reliable BER activity monitoring [31–34]. Other groups endeavored to develop fluorogenic substrates to specifically detect damaged base excision [35, 36]. Even so, the multiplexing capabilities of in-solution fluorescent probes are limited by the use of spectrally resolved fluorophores. Several biochips based on the selective immobilization of substrate oligonucleotides have been developed to monitor several BER activities by fluorescence or surface plasmon resonance [37–39]. Despite high parallelization abilities, the production of these chips is time-consuming, requires expensive equipment, and shows inter- and intra-experiment variability requiring result normalization. Here, we report the development of a BER enzymatic assay combining molecular beacon-like probes supported on microparticles (termed hereafter microbeacons, μBs) and flow cytometry readout. Signal-on and signal-off assays were first developed for the detection of DNA *N*-glycosylases, AP-endonucleases, and restriction enzymes. Next, using signal-on — profluorescent — probes, we combined the end-point readout of flow cytometry with real-time monitoring of enzymatic activities of purified proteins or cell extracts. We also adapted the assay to a multiplex format and compared it to the singleplex assay. Therapeutic inhibitors screening and DNA repair phenotyping are finally exemplified as potential applications of the bead-based biosensing technique.

Material and methods

Synthesis of DNA probes

Oligonucleotides were synthesized at the micromole scale on an automatic nucleic acid synthesizer *Applied Biosystems 392 DNA/RNA Synthesizer*, using 3'-biotinTEG or 3'-Dabcyl CPG column (Glen Research). Sequences are listed in Table S1. Phosphoramidite monomers (Pac-dA, dT, Ac-dC, Pac-dG-3'-CE phosphoramidite) and modified synthons (dU, tetrahydrofuran moiety, dabcyl-dT, cy5-dT, BHQ-2, cyanine 3, and cyanine 5) were purchased from Glen Research. At the end of the synthesis, bases and phosphates were deprotected and oligonucleotides were cleaved from the support with a solution of 30% ammonium hydroxide for 16 h at room temperature. Ammonia was removed by centrifugation under vacuum in a Speedvac® SPD 111 V. Crude oligonucleotides were pre-purified by denaturing 7 M urea polyacrylamide gel electrophoresis (1 × TBE buffer, Life Technologies, power limited to 30 W). Products were excised from the gel and eluted in ultrapure milliQ water. An additional purification was performed by reverse phase HPLC with a Hypersil® HS C18 column heated at 50 °C mounted on an Agilent Technologies 1200 series system. DNA fragments were eluted with a linear gradient of acetonitrile in 10 mM triethylammonium. Chromatography was coupled to absorbance detection at 260 nm (DNA) and 453 nm (dabcyl) or 579 nm (BHQ-2). A fluorescence module allowed the fluorophore detection of cyanine 3 (λex = 546 nm, λem = 563 nm) or of cyanine 5 (λex = 649 nm, λem = 670 nm). Collected fractions were concentrated thanks to the Speedvac®, desalted, freeze-dried, and finally solubilized in milliQ water for storage at − 20 °C. Purified oligonucleotides were dosed by absorbance with a Nanodrop ND-1000 (Thermo Scientific) and quality-checked by HPLC analysis and MALDI-ToF mass spectrometry measurements.

Immobilization of DNA probes on beads

Two types of magnetic beads were used. Streptavidin-coated magnetic beads (2.8 µm, B_A) were purchased from Life Technologies. Biotinylated microspheres (4 µm, B_B) were provided by Kisker Biotech. Streptavidin beads were used in direct conjugation with biotinylated probes. Beads B_A were first equilibrated in the 1 × Binding and Washing buffer (B&W; 5 mM Tris–HCl pH 7.5, 0.5 mM EDTA, 1 M NaCl). DNA probes were diluted at a concentration of 250 nM in 1 × B&W buffer and subjected to annealing (90 °C for 2 min followed by a gradual temperature decrease down to room temperature over 10 min). Beads were pelleted on a magnetic rack; the supernatant was removed, and the probe solution was added (60 µL for 100 µg of beads). The mixture is incubated for 1 h at room temperature under agitation in the dark. μB_A were washed three times with 1 × B&W buffer and finally resuspended in 12 µL of the digestion buffer (10 mM HEPES/KOH (pH 7.8), 2 mM EGTA/KOH (pH 7.8), 80 mM KCl, 0.1 mM $ZnCl_2$, 1 mM DTT et 0.5 mg·mL^{-1} BSA) and stored at 4 °C for up to 1 month.

Biotinylated beads B_B were coated with streptavidin prior to probes immobilization. Briefly, 10 µL of the storage vial were washed three times with 1 × B&W buffer and suspended in 5 µL of B&W buffer. Streptavidin (5 µL, 1 µg·mL^{-1} in PBS; Sigma Aldrich) was added and the mixture was incubated for 15 min at room temperature under agitation (1000 rpm). For multiplex assays, different ratios of streptavidin/Alexa488-conjugated streptavidin were used to barcode the different microbeacon populations, which were eventually distinguishable during the flow cytometry analysis. Beads were washed five times with the B&W buffer to remove the excess of streptavidin, resuspended in 25 µL of B&W buffer, followed by the addition of 15 µL of annealed DNA probe (1 µM in B&W buffer). The suspension was agitated for 1 h at room temperature in the dark. μB_B were washed 3 times with B&W buffer and resuspended in 20 µL of digestion buffer.

Cell lines and culture

LN428 (glioblastoma) cell lines were purchased from Trevigen. The transduced knockdown subline stamped "KD-APE1" stably expresses a plasmid producing a small hairpin RNA (shRNA) targeting *ape1* gene. The control cell line (KD-CTRL) expresses an empty plasmid. Cells were grown at 90% confluence in alpha-modified Dulbecco's minimum essential medium Eagle (α-MEM, Gibco), supplemented with 10% v/v heat-inactivated fetal calf serum (Gibco), 2 mM L-glutamine, 5 µg·mL^{-1} gentamicin, 0.8% of a 100 × antibiotic/antimycotic solution (Invitrogen), at 37 °C in 5% CO_2-enriched humidified atmosphere. Puromycin was added before seeding at the final concentration of 1 µg·mL^{-1}. Cells were harvested by trypsinization, counted, and aliquoted at 5.10^6 cells·mL^{-1} in α-MEM supplemented with 20% FCS and 20% DMSO (Sigma) before being stored at − 80 °C. The following day, cells were transferred in liquid nitrogen cryo-tank for long-term storage.

Nuclear extract preparation

Nuclear extracts were prepared according to a previously described method [40]. Briefly, cells were thawed on ice and washed twice with ice-cold PBS. Pellets were suspended in 1 mL ice-cold buffer A (10 mM HEPES pH 7.9, 1.5 mM $MgCl_2$, 10 mM KCl, 0.02% Triton X-100, 0.5 mM DTT, 18 µg·mL^{-1} PMSF). Nuclei are recovered by centrifugation and resuspended in 25 µL of ice-cold buffer B (10 mM HEPES pH 7.9, 1.5 mM $MgCl_2$, 400 mM KCl, 0.2 mM EDTA, 25% glycerol, 0.5 mM DTT, 0.7 × complete antiproteases cocktail (Roche) and 18 µg·mL^{-1} PMSF). The nuclear lysis proceeded for 20 min at 4 °C and was completed by two freezing–thawing cycles at − 80 °C and 4 °C, respectively. The extracts were cleared by centrifugation (10 min, 16,000 *g*, 4 °C). Lysates were stored at − 80 °C and thawed on ice prior to experiments. Protein concentration was determined by Micro BCA assay (Interchim), and calibrated by standard solutions of bovine serum albumin, according to the provider's instruction. HeLa nuclear extracts were purchased from CIL Biotech, aliquoted at 9 µg·µL^{-1} and stored at − 80 °C.

Enzymatic digestion

Uracil-DNA glycosylase (UDG), purified from *Escherichia coli, human Alkyl Adenine DNA glycosylase* and human AP-endonuclease 1 (APE1), were purchased from New England Biolabs (NEB). The restriction enzyme Pst1 and the corresponding buffer were provided by Trevigen. Purified enzyme(s) or nuclear extract and the corresponding 1 × enzymatic buffer (digestion buffer, except for Pst1, performed in 50 mM Tris–HCl, 10 mM $MgCl_2$, 50 mM NaCl, pH 7.8) were added to 1 µL of µB and the digestion proceeded for 1 h at 37 °C. Real-time monitoring was conducted in a thermocycler Stratagene Mx3000p (Agilent Technologies), set at a constant temperature of 37 °C. Due to the relatively large colloid size (2.8 µm for the μB_A, 4 µm for the μB_B), µB are expected to slowly sediment during the time of the reaction. Following incubation, 200 µL of cold PBS supplemented with 0.02% Tween 20 were added to quench the enzymatic reactions.

Flow cytometry and analysis

Flow cytometry analysis was conducted on a FACSCalibur instrument (Becton Dickinson). A minimum of 10^4 events per sample were collected. Data were processed with FCS-express software (De Novo Software) and arithmetic medians were used to quantify cleavage rate. Signal-to-noise ratios (SNRs) were calculated according to the formula

$$SNR = F_{max}/F_{min}$$

where F_{max} and F_{min} correspond to the maximum (i.e., the negative control with no enzyme for the µB-F and the positive control with the highest enzyme concentration for µB-Q) and minimum (i.e., the negative control with no enzyme for the µB-Q and the positive control with the highest enzyme concentration for µB-F) fluorescence intensities, respectively.

Polyacrylamide gel electrophoresis

Polyacrylamide gel electrophoresis (PAGE) was performed from 1 µL of in-solution probe (1 µM, annealed in the corresponding buffer). After digestion (final volume 10 µL), 3 µL of formamide blue (90% formamide, 0.02% xylene cyanol, 0.02% bromophenol) were added and samples were heated for 3 min at 90 °C before being deposed on a 20% v/v acrylamide gel with 7 M urea. Migration was carried out with 1 × Tris/Borate/EDTA buffer (TBE 10 ×, Life Technologies). Gels were imaged on a fluorescence scanner Typhoon ™ 9400 (GE Healthcare).

Results and discussion

Signal-on versus signal-off strategies

The reported biosensor relies on microbeads functionalized with modified oligonucleotide probes each targeting a specific enzymatic activity. We first compared two detection approaches: the signal-off strategy, using fluorescent probes; the signal-on strategy, employing profluorescent molecular beacon-like probes (Fig. 1A). In the signal-off configuration, oligonucleotides (ODN-F) are 5'-labeled with a fluorophore (cyanine3) and 3'-biotinylated. Probe's cleavage causes the release of the fluorescent moiety in the supernatant and as a result the decrease of beads' fluorescence. In the signal-on approach, hairpin-shaped oligonucleotides (ODN-Q) are dual-labeled with a fluorophore (proximal to the biotin) and a quencher (opposite to the fluorophore) pair. In its initial configuration, the probe exhibits a minimum of fluorescence. Stem cleavage leads to the dehybridization of the fragment containing the quencher and restores fluorescence emission at the bead surface. The two strategies were first tested using purified enzymes: a restriction enzyme, Pst1, acting on the Pst1-F and Pst1-Q probes, which contain the restriction site in the stem; an AP-endonuclease, APE1, cleaving the AP-site analogue tetrahydrofuran (THF) inserted in the THF-F and THF-Q probes [41, 42], and a DNA *N*-glycosylase, alkyladenine DNA glycosylase (AAG), which excises deaminated adenine (hypoxanthine, Hx) in Hx-F, Hx-Q, leaving an abasic site revealed by additional APE1 cleavage.

Streptavidin-coated particles (μB_A) were functionalized with each of the six probes (μB_A-Pst1-F, μB_A-Pst1-Q, μB_A-THF-F, μB_A-THF-Q, μB_A-Hx-F, μB_A-Hx-Q) and incubated with an increasing concentration of the targeted purified enzyme(s). Flow cytometry analyses after 1 h at 37 °C are reported in Fig. 1B and Figure S1. The gaussian repartition of values for each bead population shows uniform probe digestion at the bead surface. SNRs were computed to quantitatively compare the two strategies (Fig. 1C and "Material and methods" section for the calculation). For μB_A-Pst1, F and Q probes yield identical SNRs (4.5 ± 0.3). For μB_A-THF and μB_A-Hx, signal-off strategy exhibits a significantly higher SNR (μB_A-THF-F = 3.8 ± 0.2 vs 2.6 ± 0.5 for μB_A-THF-Q; μB_A-Hx-F = 4.8 ± 0.2 vs 2.3 ± 0.3 for μB_A-Hx-Q). The lower SNRs in the signal-on strategy can be explained by the quenching efficiency (< 1), which results in a substantial initial fluorescence background. The signal-off strategy, however, relies on the cleavage of the fluorophore off the particle with a final background that corresponds to the particle autofluorescence. The variability of the SNR for different probes suggests that this parameter is also influenced by the quality of the oligonucleotide, including the integrity of fluorophore and quencher and purity of the probes [43].

Microbeacon optimization

The signal-off strategy has the benefit of being cost-efficient because it requires the modification of the probe with a single dye, as opposed to signal-on approach that needs both an internal fluorophore and a quencher. In addition, signal-to-noise ratios are expected to be higher for signal-off assays due to the uncomplete quenching efficiency in quenched microbeacons. However, the signal-on strategy allows real-time monitoring of DNA cleavage as the fluorescence is generated from the dehybridization of the quencher moiety — whereas the signal-off approach solely involves the relocalization of the fluorescent moiety from the bead to the supernatant, with no change in the number of emitting fluorophores. We therefore focused assay optimizations on the signal-on strategy. We first assessed

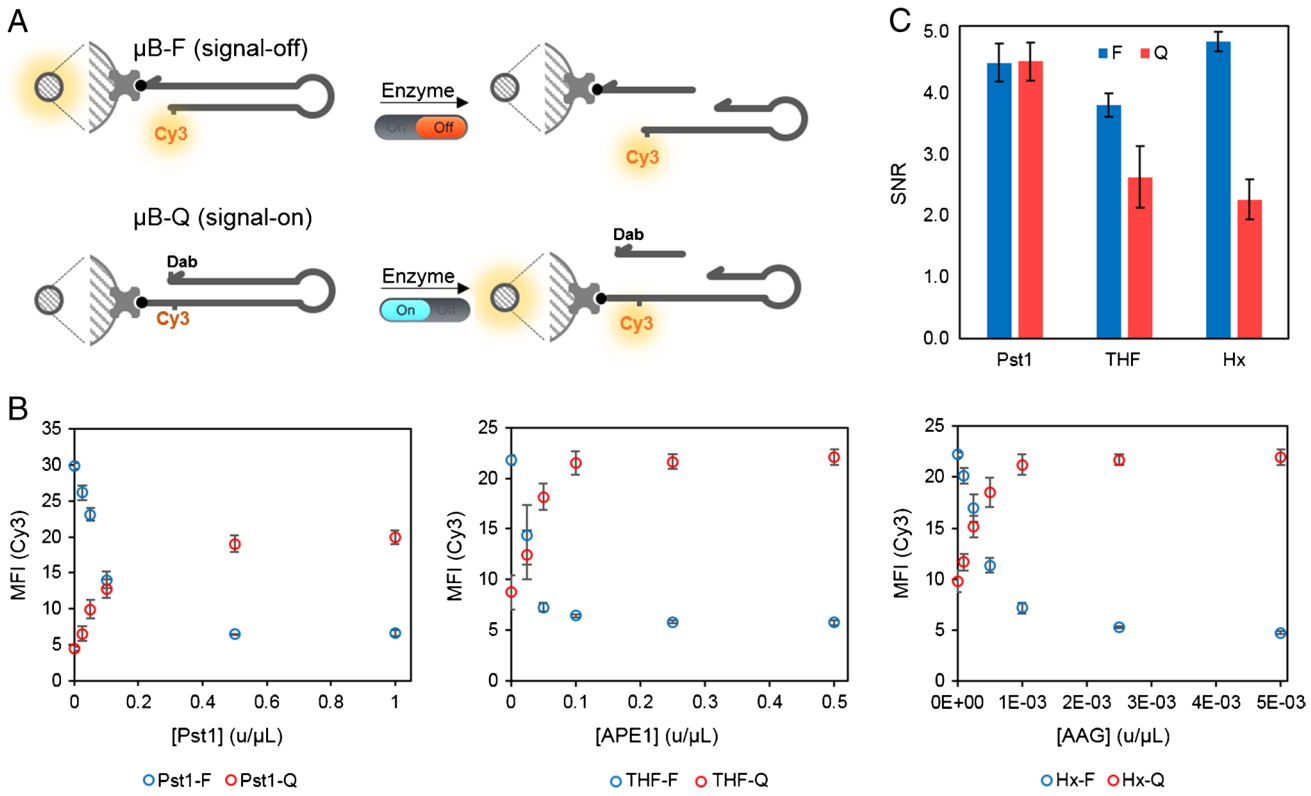

Fig. 1 Microbeacons (μB) to monitor BER activities. **A** Hairpin-shaped oligonucleotides are modified to include the substrate of the targeted enzymatic activity. The signal-off strategy uses μB-F functionalized with a fluorescent probe whose fluorescence fragment is released off the bead after cleavage resulting in a decrease of the bead's fluorescence. The signal-on strategy uses μB-Q functionalized with a dual-labeled profluorescent probe whose quencher fragment is released off the bead after cleavage inducing an increase in bead fluorescence. **B** Flow cytometry analysis of μB-F (blue circle) or μB-Q (red circle) incubated in presence of a varying concentration of the targeted enzyme, Pst1, APE1, or AAG. Mean fluorescence intensities and standard deviations from 3 independent duplicate experiments. **C** Comparison of the signal-to-noise ratio (SNR) for the signal-off (F) and on (Q) approaches

the effect of chromophores: the substitution of Cy3 by Cy5 (probes Pst1-Q2, THF-Q2) did not increase the SNR, as the quenching efficiency of the dabcyl was only 76%. However, the pair Cy5/BHQ2 allowed to increase the SNR by 1 order of magnitude (46.6 ± 6.5 and 27.0 ± 4.6 for μB_A-Pst1-Q3 and μB_A-THF-Q3, respectively) (Figure S2). These SNR values are comparable to both in-solution molecular beacons for AP-endonuclease and DNA *N*-glycosylase detection [34, 44] and on-beads molecular beacons for nucleic acid detection [45]. The difference between the two Q3 probes may be explained by the utilization of a deoxythymidine-conjugated cyanine 5 phosphoramidite (Cy5-dT) to synthesize the probe Pst1-Q3 while the Cy5 phosphoramidite was used for other Q3 probes (Figure S3). In the first case, the flexibility provided by the linker between the thymine and the fluorophore promotes the exciton interaction between the two dyes, ideal for contact quenching [43]. In contrast, the rigidity of the Cy5 synthon tethered by both extremities of the dye may prevent optimal interaction between the two chromophores.

The influence of the bead's size and type was also evaluated. We compared 2.8 μm streptavidin beads (μB_A) with 4 μm biotinylated paramagnetic beads (μB_B) (Figure S4). In the latter case, biotin-modified probes were tethered by bridging streptavidin (cf. experimental section). It has been previously shown that this strategy leads to a further increase of the signal-to-noise ratio upon hybridization of a nucleic acid target by comparison to direct immobilization of probes to streptavidin-conjugated microbead [45]. The SNR for the THF-Q3 probe is comparable for both microbeacons (25.3 ± 3.7 and 25.6 ± 3.4 for μB_A-THF-Q3 and μB_B-THF-Q3, respectively). Interestingly, μB_B-Pst1-Q3 exhibits a SNR > 200, i.e., 4.6 times higher than its μB_A counterpart. It is to note that the maximal MFI is multiplied by a factor 1.8 ± 0.07.

Real-time monitoring of purified enzymatic activities combined with end-point flow cytometry

To extend the biosensor to the detection of another DNA glycosylase, we synthesized a uracil-containing DNA probe, Ura-Q3 (Table S1). Uracil in DNA is specifically recognized by the well-conserved uracil DNA glycosylase

(bacterial UDG or the human homolog UNG) [16, 46]. Here, the activity of the restriction enzyme Pst1, the AP-endonuclease APE1, and the bacterial UDG is studied. Corresponding μB_B were digested with purified enzymes Pst1, APE1, or UDG (the latter supplemented with 1 unit of APE1 to reveal AP-sites resulting from the glycosylase activity), respectively. Probes cleavage is monitored in real-time in a thermocycler set at 37 °C (Figure 2A). First, we noticed the steadiness of the signal in absence of enzymes, proving the high quenching stability over time. The initial speed is positively correlated to the enzyme concentration. Flow cytometry analyses validated the relationship between the response of the biosensor and the initial enzyme concentration (Figure 2B). The standard deviation calculated for positive controls (with the highest enzyme concentration) is below 10%, demonstrating the high reproducibility and repeatability of the detection technique. Confirmation of probes specificity is given by electrophoresis analysis of the in-solution probes incubated with the enzymes UDG and APE1 (Figure S5).

The limit of detection for UDG is around 5 10^{-5} unit, namely 5 10^{-3} u·mL^{-1}. A study reports the detection of the same enzyme by an electrochemical biosensor, exhibiting a comparable detection limit with 8 10^{-3} u·mL^{-1} [47]. Tao et al. reported the detection of 8 10^{-4} u·mL^{-1} of UDG [48]. This method relies on an artificial non-base spacer that is quenched by uracil, hence restricting the assay to the detection of uracil glycosylases.

Detection of BER activities in cell extract

The ability of microbeacons to detect DNA repair activities in cell extract was then investigated. The main limitation of the use of molecular beacons in homogeneous assays comes from their degradation in cell extract, mainly by 3'-exonucleases [49, 50]. Although chemical modifications such as phosphorothioate, 2'-O-methyl-ribose can be introduced within DNA, we previously showed that the 3'-tethering of nucleic probes to magnetic beads quantitatively limits the nonspecific degradation within biological samples [51]. This was confirmed here using μB_A-Pst1-Q with a reversed orientation (3' biotin moiety and 5' quencher, Figure S6). When oligonucleotides were anchored by a 5' biotin, the probe is prone to nonspecific degradation leading to its quantitative unquenching. On the contrary, when attached from its 3' end, no significant degradation was observed with up to 1 mg·mL^{-1} of cell extract.

μB_B-ODN-Q3 were incubated with a concentration of nuclear extract obtained from HeLa cells ranging from 0 to 50 µg of total proteins·mL^{-1}. Real-time measurements (Figure 3A) were followed by the flow cytometry analysis of the particles (Figure 3B). As expected from previous

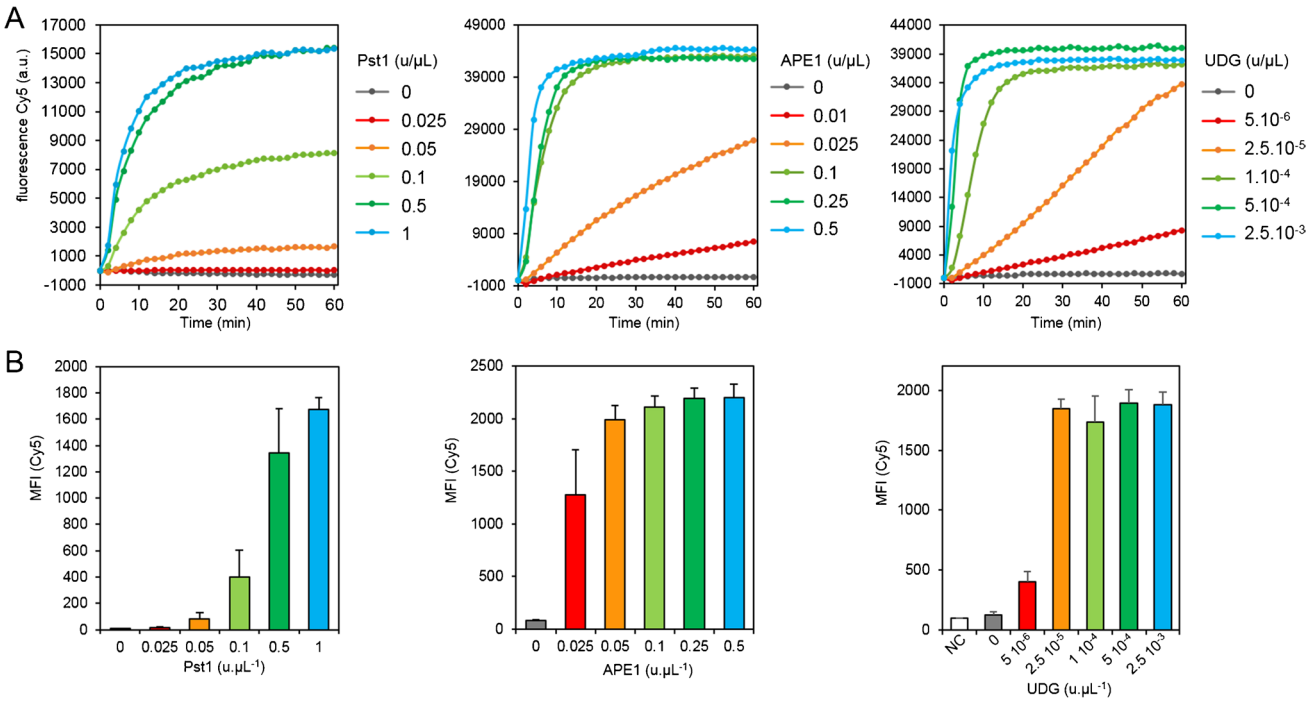

Fig. 2 Detection of purified Pst1, APE1, and UDG activities using µB-Pst1-Q3, µB-THF-Q3, and µB-Ura-Q3, respectively. **A** Real-time monitoring of the enzymatic cleavage at 37 °C for various enzyme concentrations. **B** Flow cytometry analysis of µB-Q3 fluorescence after 1 h of incubation. Error bars correspond to 3 independent experiments performed in duplicate

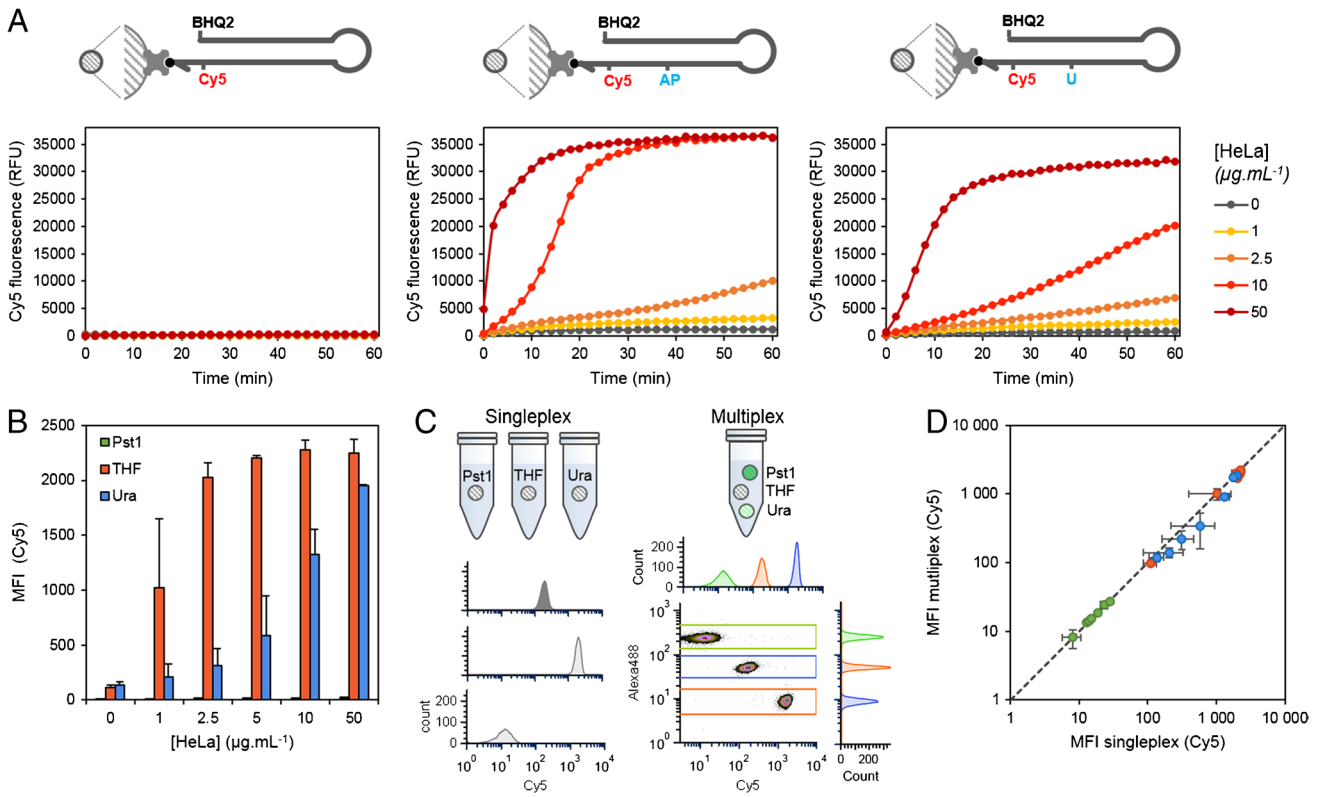

Fig. 3 BER enzyme detection from HeLa nuclear extract. **A** Real-time monitoring followed by **B** flow cytometry analysis of μBB-Q3 in presence of an increasing concentration of nuclear proteins (singleplex format). **C** Singleplex versus multiplex assay. In the multiplex format, μB are encoded with distinguishable ratios of Alexa488-conjugated and non-fluorescent streptavidin. **D** Comparative analysis of singleplex versus multiplex assay (extended data in Figure S7). For μBB-Pst1-Q3, THF-Q3, and Ura-Q3, a linear fit gives $y=1.00x$ ($R^2=0.99$), $y=0.94x$ ($R^2=0.97$), and $y=0.89x$ ($R^2=0.95$), respectively

observations, μB_B-Pst1-Q3 (with no lesion, used as a negative control) remains non-fluorescent, even at the highest protein concentration, confirming that 3' tethering of the probe increases its stability in complex media.

Real-time monitoring of both damaged probes showed a faster digestion kinetic for THF-Q3 than Ura-Q3, in agreement with previous studies using mammalian [34] or drosophila cells [52]. The detection limit of uracil glycosylase was 5 μg proteins·mL^{-1}, in the experimental conditions. APE1 was detected from 1 μg·mL^{-1} (i.e., 10 ng of proteins per sample), consistent with a previous study that reported a limit of detection close to 5 μg·mL^{-1} of proteins [53].

Singleplex to multiplex assay

According to a method previously described [54], we run the assay in a multiplex format for the detection of APE1 and UNG in HeLa cell extract (including a negative control with the Pst1-Q3 probe) and compared it to the results singleplex format (Figure 3C). In the multiplex assay, particles B are encoded with different ratios of fluorescently labeled and non-fluorescent streptavidin, distinguishable by flow cytometry (Figure S7). Each particle type is then functionalized with one of the Q3 probes (THF, Ura, or Pst1 as a control) allowing for the simultaneous detection of APE1 and UNG. As observed in Figure 3D, there is an almost perfect correlation between the singleplex and multiplex measurements, with the exception of the Ura-Q3 probe, which gives a lower signal in the multiplex format for intermediate concentration. This translates in a slight deviation from the diagonal. This result can be explained by the requirement of both UNG and APE1 for the cleavage of the Ura-Q3 probe: APE1 being also requested for the cleavage of THF-Q3 probe, this may result in a competitive inhibition of the μB_B-Ura-Q3 cleavage in multiplex format with μB_B-THF-Q3. Nevertheless, as compared to the parallelized singleplex assay (where each μB is incubated and analyzed separately), the multiplex format requires less sample volume, less consumables, and is time and cost-saving.

Analysis of UDG inhibitor

Using the multiplex format, we further demonstrated the possibility to detect specific enzyme inhibitors (Figure 4A). As a model, we selected the uracil glycosylase inhibitor (UGI), a well-known inhibitor of UNG. It is a monomeric protein of 9474 Daltons produced by *Bacillus subtilis* bacteriophages PBS-1 and PBS-2. UGI tightly binds the DNA binding site of UNG to form a stable 1:1 complex that is essentially irreversible under physiological conditions [55]. We first confirmed the specific inhibition of the uracil *N*-glycosylase using purified bacterial UDG (Figure S8). The specificity of UGI for the human homolog from cell-free extract was then investigated. 50 $\mu g \cdot mL^{-1}$ of HeLa nuclear extract were preincubated with an increasing amount of UGI before being exposed to fluorescently encoded μB_B-Pst1-Q3, μB_B-THF-Q3, and μB_B-Ura-Q3. Flow cytometry analyses show the decrease in fluorescence intensity solely of Ura-Q3 supported particles (Figure 4B–C). We observed a sharp transition of the inhibition between 5.10^{-6} and $2.5.10^{-5}$ $u \cdot \mu L^{-1}$, in accordance with the suicide inhibitory mechanism of UGI that forms a quasi-irreversible complex with UNG under physiological conditions [55]. For all UGI concentrations, the signal of μB_B-THF-Q3 remained maximal. As in previous experiments, μB_B-Pst1-Q3 was stable and exhibited a minimum fluorescent signal. Conjointly, these observations validate the specificity of the cleavage by DNA repair enzymes and of the inhibition of uracil glycosylase by UGI.

Microbeacons for the discrimination of cell line APE1 phenotype

Measuring DNA repair activities in tumor tissues represents a promising strategy to assess the best treatment opportunities, either for bypassing proficient repair mechanisms (that lead to tumor resistance) or on the

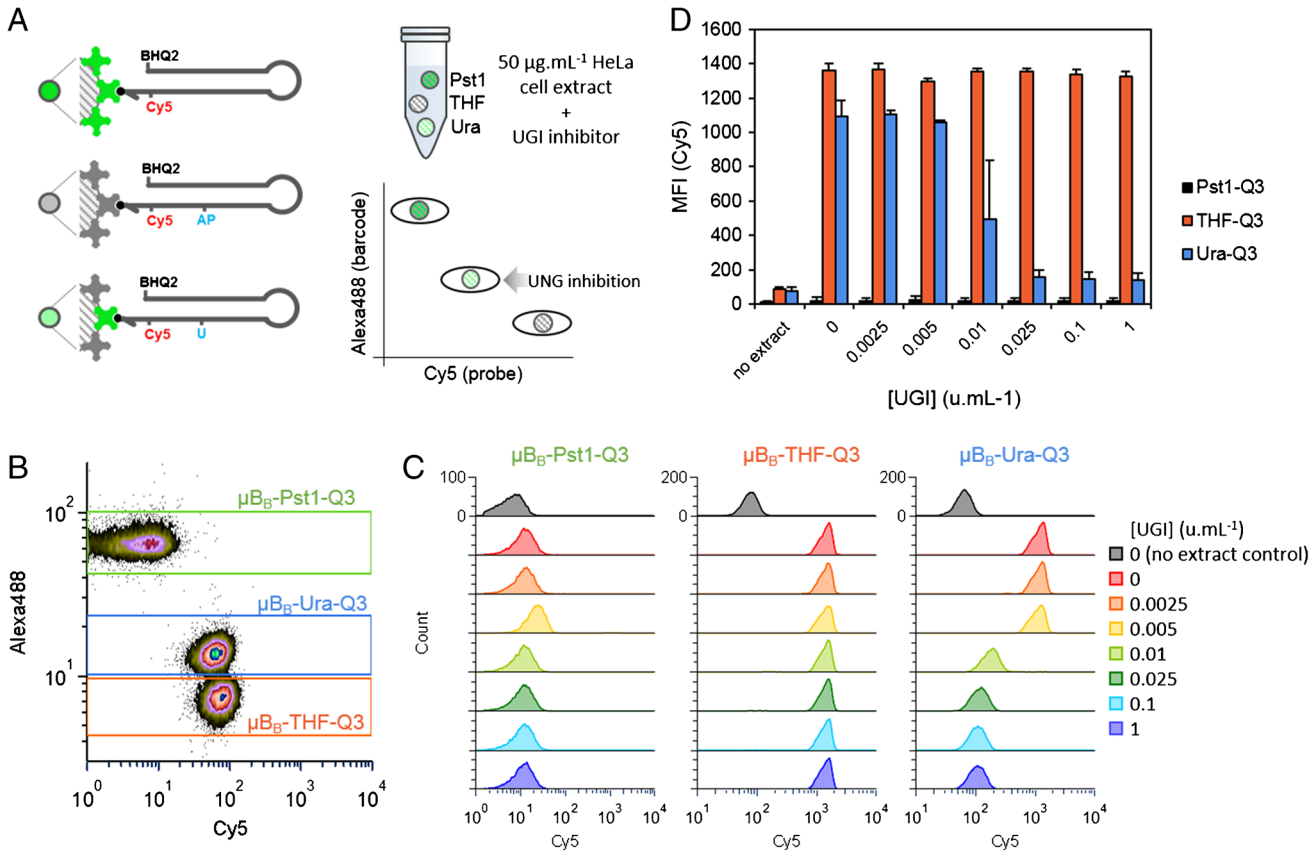

Fig. 4 Uracil *N*-glycosylase inhibition by uracil glycosylase inhibitor (UGI). **A** Multiplex assay using fluorescently encoded µB. μB_B-Pst1-Q3, THF-Q3, and Ura-Q3 are incubated with 50 $\mu g \cdot mL^{-1}$ of HeLa cell extract preincubated 10 min at room temperature with various concentrations of UGI. **B** Representative 2D histogram of the Alexa488 barcode/Cy5 probe fluorescence (no extract control sample). **C** Flow cytometry histograms of the µB fluorescence after 1 h of incubation at 37 °C. **D** Flow cytometry analysis. Error bars correspond to 3 independent experiments performed in duplicate

contrary leverage enzymatic deficiencies. As a proof of principle, APE1 activity was measured in APE1 knockdown cells ("KD-APE1," expressing a shRNA targeting *ape1*) and control cells ("KD-CTRL," transfected with an empty plasmid). μB_B-THF-Q3 was incubated with nuclear extract prepared from both sublines ranging from 0 to 5 $\mu g \cdot mL^{-1}$ or proteins. Real-time monitoring of APE1 (Figure 5A–B) demonstrated the dose-dependency between the concentration of proteins and the probes digestion kinetic. It established a twofold decrease in activity within the KD-APE1 cell line compared to the control cell line. Similarly, end-point flow cytometry analysis reveals a significantly reduced APE1 activity at 2.5 $\mu g \cdot mL^{-1}$ or less (Figure 5C). At 5 $\mu g \cdot mL^{-1}$ however, no difference was observed between the two cell lines, due to the quantitative probe digestion. This observation demonstrates the complementarity of real-time monitoring and end-point single-bead analysis by flow cytometry (Figure 5D).

Conclusion

In this work, we developed a bead-based assay for BER enzyme detection. It combines the convenience and reproducibility of grafting streptavidin-conjugated microspheres with the stability and robustness of flow cytometry apparatus, ensuring high inter-experiment reproducibility without requiring normalization. In addition, the encoding of the particles by fluorescence intensity (among other means [45, 56]) enables to straightforwardly multiplex the assay using a set of probes all modified with the same fluorescent dye.

The profluorescent character of Q-probe used in the signal-on approach authorizes real-time detection of enzymatic activities, which ought to provide a fast way to adjust digestion time and temperature and optimize assay conditions with respect to the application. Such complementary analysis enables to improve results significance obtained by flow cytometry (Fig. 5C).

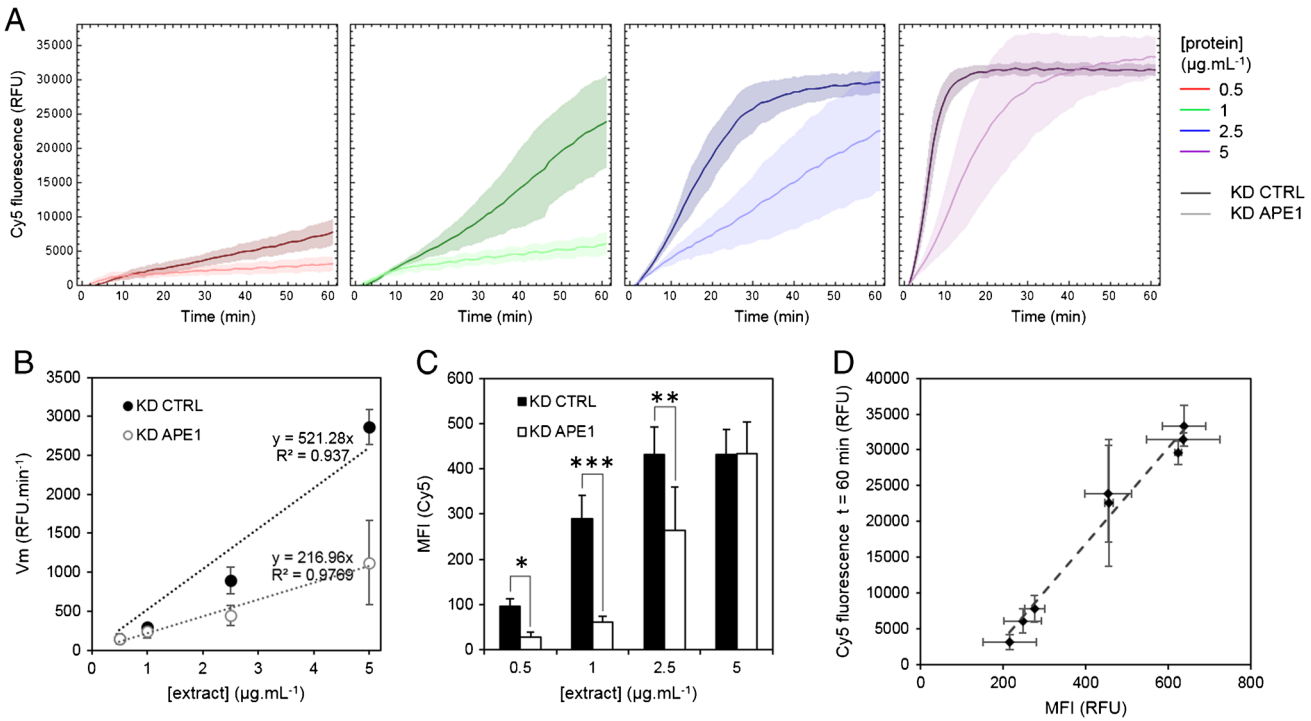

Fig. 5 Discrimination of APE1 activity within two cell sublines. The p53 deficient glioblastoma cell line LN428 was transfected with a plasmid stably expressing a shRNA targeting the gene ape1 or an empty plasmid, establishing the sublines KD-APE1 and KD-CTRL, respectively. **A** Real-time monitoring of APE1 activity at (from left to right) 0.5, 1, 2.5, and 5 $\mu g \cdot mL^{-1}$ of nuclear proteins with µBB-THF-Q3. Time traces were normalized by the negative control sample (0 $\mu g \cdot mL^{-1}$ protein). Shades represent the standard deviation based on 3 independent experiments in duplicate. **B** Initial cleavage velocity was plotted as a function of the protein extract concentration. Dashed lines represent the linear regression. **C** End-point flow cytometry analysis of µB-THF-Q3 after 1 h of incubation at 37 °C (✱ $p < 0.1$, ✱✱ $p < 0.05$, ✱✱✱ $p < 0.001$ ANOVA test). **D** End-point signal correlation between thermocycler measurement ($t = 60$ min from the real-time monitoring) and flow cytometry analysis

The use of microbeacons coupled to a classic flow cytometry analysis has proved to be well-suited to detect various enzymatic activities such as base excision repair enzymes but also restriction enzymes and various nucleases in a fast and specific manner. The sensitivity could be improved by combining microbeacons with an isothermal amplification mechanism [57–61]. The amplification-free nature of the assay, however, allowed the robust detection of BER activities from crude cellular extracts. Relying on high-throughput flow cytometry technology, this tool is suitable to discover new DNA repair inhibitors that can be used to potentiate current cancer treatments. Likewise, the monitoring of patient enzymatic status represents an attractive strategy to tailor cancer treatment accordingly.

Current works are led to improve the multiplexing and parallelizing ability of this tool so that inhibitor screening of various base excision repair actors can be developed.

Supplementary Information The online version contains supplementary material available at https://doi.org/10.1007/s00216-021-03849-9.

Acknowledgements The authors would like to thank Yannick Rondelez for the careful proofreading of the manuscript.

Author contribution DG acquired funds. DG and GG designed the study. GG, CB, and CSP performed experiments and analyzed the data. DG and GG wrote the manuscript.

Funding This work was supported by the thesis funding program of CEA and the French National Research Agency (Labex ARCANE and CBH-EURGS, ANR-17-EURE-0003).

Availability of data and material All data are available upon reasonable request.

Declarations

Consent for publication All authors have given approval to the final version of the manuscript.

Competing interests The authors declare no competing interests.

References

1. Burrows CJ, Muller JG. Oxidative nucleobase modifications leading to strand scission. Chem Rev. 1998;98:1109–52. https://doi.org/10.1021/cr960421s.
2. Cadet J, Douki T, Gasparutto D, Ravanat J-L. Oxidative damage to DNA: formation, measurement and biochemical features. Mutation Research/Fundamental and Molecular Mechanisms of Mutagenesis. 2003;531:5–23. https://doi.org/10.1016/j.mrfmmm.2003.09.001.
3. Gates KS. An overview of chemical processes that damage cellular DNA: spontaneous hydrolysis, alkylation, and reactions with radicals. Chem Res Toxicol. 2009;22:1747–60. https://doi.org/10.1021/tx900242k.
4. Chatterjee N, Walker GC. Mechanisms of DNA damage, repair and mutagenesis. Environ Mol Mutagen. 2017;58:235–63. https://doi.org/10.1002/em.22087.
5. Hoeijmakers JH. Genome maintenance mechanisms for preventing cancer. Nature. 2001;411:366–74. https://doi.org/10.1038/35077232.
6. Al-Tassan N, Chmiel NH, Maynard J, Fleming N, Livingston AL, Williams GT, Hodges AK, Davies DR, David SS, Sampson JR, Cheadle JP. Inherited variants of MYH associated with somatic G:C→T: A mutations in colorectal tumors. Nat Genet. 2002;30:227–32. https://doi.org/10.1038/ng828.
7. Wallace SS, Murphy DL, Sweasy JB. Base excision repair and cancer. Cancer Lett. 2012;327:73–89. https://doi.org/10.1016/j.canlet.2011.12.038.
8. Rapin I, Lindenbaum Y, Dickson DW, Kraemer KH, Robbins JH. Cockayne syndrome and xeroderma pigmentosum. Neurology. 2000;55:1442–9.
9. Dixon K, Kopras E. Genetic alterations and DNA repair in human carcinogenesis. Semin Cancer Biol. 2004;14:441–8. https://doi.org/10.1016/j.semcancer.2004.06.007.
10. Trivedi RN, Almeida KH, Fornsaglio JL, Schamus S, Sobol RW. The role of base excision repair in the sensitivity and resistance to temozolomide-mediated cell death. Cancer Res. 2005;65:6394–400. https://doi.org/10.1158/0008-5472.CAN-05-0715.
11. Damia G, Broggini M. Platinum resistance in ovarian cancer: role of DNA repair. Cancers. 2019;11:119. https://doi.org/10.3390/cancers11010119.
12. Paik J, Duncan T, Lindahl T, Sedgwick B. Sensitization of human carcinoma cells to alkylating agents by small interfering RNA suppression of 3-alkyladenine-DNA glycosylase. Can Res. 2005. https://doi.org/10.1158/0008-5472.CAN-05-1495.
13. Visnes T, Grube M, Hanna BMF, Benitez-Buelga C, Cázares-Körner A, Helleday T. Targeting BER enzymes in cancer therapy. DNA Repair. 2018;71:118–26. https://doi.org/10.1016/j.dnarep.2018.08.015.
14. Martin SA, Lord CJ, Ashworth A. DNA repair deficiency as a therapeutic target in cancer. Curr Opin Genet Dev. 2008;18:80–6. https://doi.org/10.1016/j.gde.2008.01.016.
15. Robertson AB, Klungland A, Rognes T, Leiros I. DNA repair in mammalian cells: base excision repair: the long and short of it. Cell Mol Life Sci. 2009;66:981–93. https://doi.org/10.1007/s00018-009-8736-z.
16. Lindahl T. An N-glycosidase from Escherichia coli that releases free uracil from DNA containing deaminated cytosine residues. Proc Natl Acad Sci U S A. 1974;71:3649–53. https://doi.org/10.1073/pnas.71.9.3649.
17. Imai K, Slupphaug G, Lee W-I, Revy P, Nonoyama S, Catalan N, Yel L, Forveille M, Kavli B, Krokan HE, Ochs HD, Fischer A, Durandy A. Human uracil–DNA glycosylase deficiency associated with profoundly impaired immunoglobulin class-switch recombination. Nat Immunol. 2003;4:1023–8. https://doi.org/10.1038/ni974.
18. Kavli B, Andersen S, Otterlei M, Liabakk NB, Imai K, Fischer A, Durandy A, Krokan HE, Slupphaug G. B cells from hyper-IgM patients carrying UNG mutations lack ability to remove uracil from ssDNA and have elevated genomic uracil. J Exp Med. 2005;201:2011–21. https://doi.org/10.1084/jem.20050042.
19. Date H, Onodera O, Tanaka H, Iwabuchi K, Uekawa K, Igarashi S, Koike R, Hiroi T, Yuasa T, Awaya Y, Sakai T, Takahashi T, Nagatomo H, Sekijima Y, Kawachi I, Takiyama Y, Nishizawa M,

Fukuhara N, Saito K, Sugano S, Tsuji S. Early-onset ataxia with ocular motor apraxia and hypoalbuminemia is caused by mutations in a new HIT superfamily gene. Nat Genet. 2001;29:184–8. https://doi.org/10.1038/ng1001-184.
20. Moreira M-C, Barbot C, Tachi N, Kozuka N, Uchida E, Gibson T, Mendonça P, Costa M, Barros J, Yanagisawa T, Watanabe M, Ikeda Y, Aoki M, Nagata T, Coutinho P, Sequeiros J, Koenig M. The gene mutated in ataxia-ocular apraxia 1 encodes the new HIT/Zn-finger protein aprataxin. Nat Genet. 2001;29:189–93. https://doi.org/10.1038/ng1001-189.
21. Chaim IA, Nagel ZD, Jordan JJ, Mazzucato P, Ngo LP, Samson LD. In vivo measurements of interindividual differences in DNA glycosylases and APE1 activities. PNAS. 2017;114:E10379–88. https://doi.org/10.1073/pnas.1712032114.
22. Figueroa-González G, Pérez-Plasencia C. Strategies for the evaluation of DNA damage and repair mechanisms in cancer. Oncol Lett. 2017;13:3982–8. https://doi.org/10.3892/ol.2017.6002.
23. Mechetin GV, Endutkin AV, Diatlova EA, Zharkov DO. Inhibitors of DNA glycosylases as prospective drugs. Int J Mol Sci. 2020;21:3118. https://doi.org/10.3390/ijms21093118.
24. Gasparutto D, Bourdat A-G, D'Ham C, Duarte V, Romieu A, Cadet J. Repair and replication of oxidized DNA bases using modified oligodeoxyribonucleotides. Biochimie. 2000;82:19–24. https://doi.org/10.1016/S0300-9084(00)00347-3.
25. Gasparutto D, Dhérin C, Boiteux S, Cadet J. Excision of 8-methylguanine site-specifically incorporated into oligonucleotide substrates by the AlkA protein of Escherichia coli. DNA Repair (Amst). 2002;1:437–47. https://doi.org/10.1016/s1568-7864(02)00016-2.
26. Vik ES, Alseth I, Forsbring M, Helle IH, Morland I, Luna L, Bjørås M, Dalhus B. Biochemical mapping of human NEIL1 DNA glycosylase and AP lyase activities. DNA Repair. 2012;11:766–73. https://doi.org/10.1016/j.dnarep.2012.07.002.
27. Tchou J, Kasai H, Shibutani S, Chung MH, Laval J, Grollman AP, Nishimura S. 8-oxoguanine (8-hydroxyguanine) DNA glycosylase and its substrate specificity. Proc Natl Acad Sci U S A. 1991;88:4690–4.
28. Dianov G, Lindahl T. Preferential recognition of I.T base-pairs in the initiation of excision-repair by hypoxanthine-DNA glycosylase. Nucleic Acids Res. 1991;19:3829–33.
29. Tyagi S, Kramer FR. Molecular beacons: probes that fluoresce upon hybridization. Nat Biotechnol. 1996;14:303–8. https://doi.org/10.1038/nbt0396-303.
30. Li J, Svilar D, McClellan S, Kim J-H, Ahn E-YE, Vens C, Wilson DM, Sobol RW. DNA repair molecular beacon assay: a platform for real-time functional analysis of cellular DNA repair capacity. Oncotarget. 2018;9:31719–43. https://doi.org/10.18632/oncotarget.25859.
31. Kundu LM, Burgdorf LT, Kleiner O, Batschauer A, Carell T. Cleavable substrate containing molecular beacons for the quantification of DNA-photolyase activity. ChemBioChem. 2002;3:1053–60. https://doi.org/10.1002/1439-7633(20021104)3:11%3c1053::AID-CBIC1053%3e3.0.CO;2-#.
32. Matsumoto N, Toga T, Hayashi R, Sugasawa K, Katayanagi K, Ide H, Kuraoka I, Iwai S. Fluorescent probes for the analysis of DNA strand scission in base excision repair. Nucleic Acids Res. 2010;38:e101. https://doi.org/10.1093/nar/gkq022.
33. Mirbahai L, Kershaw RM, Green RM, Hayden RE, Meldrum RA, Hodges NJ. Use of a molecular beacon to track the activity of base excision repair protein OGG1 in live cells. DNA Repair (Amst). 2010;9:144–52. https://doi.org/10.1016/j.dnarep.2009.11.009.
34. Maksimenko A, Ishchenko AA, Sanz G, Laval J, Elder RH, Saparbaev MK. A molecular beacon assay for measuring base excision repair activities. Biochem Biophys Res Commun. 2004;319:240–6. https://doi.org/10.1016/j.bbrc.2004.04.179.
35. Ono T, Wang S, Koo C-K, Engstrom L, David SS, Kool ET. Direct fluorescence monitoring of DNA base excision repair. Angew Chem Int Ed. 2012;51:1689–92. https://doi.org/10.1002/anie.201108135.
36. Edwards SK, Ono T, Wang S, Jiang W, Franzini RM, Jung JW, Chan KM, Kool ET. In vitro fluorogenic real-time assay of the repair of oxidative DNA damage. ChemBioChem. 2015;16:1637–46. https://doi.org/10.1002/cbic.201500184.
37. Sauvaigo S, Guerniou V, Rapin D, Gasparutto D, Caillat S, Favier A. An oligonucleotide microarray for the monitoring of repair enzyme activity toward different DNA base damage. Anal Biochem. 2004;333:182–92. https://doi.org/10.1016/j.ab.2004.06.046.
38. Flaender M, Costa G, Nonglaton G, Saint-Pierre C, Gasparutto D. A DNA array based on clickable lesion-containing hairpin probes for multiplexed detection of base excision repair activities. Analyst. 2016;141:6208–16. https://doi.org/10.1039/C6AN01165A.
39. Corne C, Fiche J-B, Gasparutto D, Cunin V, Suraniti E, Buhot A, Fuchs J, Calemczuk R, Livache T, Favier A. SPR imaging for label-free multiplexed analyses of DNA N-glycosylase interactions with damaged DNA duplexes. Analyst. 2008;133:1036–45. https://doi.org/10.1039/b801086b.
40. Millau J-F, Raffin A-L, Caillat S, Claudet C, Arras G, Ugolin N, Douki T, Ravanat J-L, Breton J, Oddos T, Dumontet C, Sarasin A, Chevillard S, Favier A, Sauvaigo S. A microarray to measure repair of damaged plasmids by cell lysates. Lab Chip. 2008;8:1713–22. https://doi.org/10.1039/B806634E.
41. Mundle ST, Delaney JC, Essigmann JM, Strauss PR. Enzymatic mechanism of human apurinic/apyrimidinic endonuclease against a THF AP site model substrate. Biochemistry. 2009;48:19–26. https://doi.org/10.1021/bi8016137.
42. Wilson DM, Takeshita M, Grollman AP, Demple B. Incision activity of human apurinic endonuclease (Ape) at abasic site analogs in DNA. J Biol Chem. 1995;270:16002–7. https://doi.org/10.1074/jbc.270.27.16002.
43. Bernacchi S, Mély Y. Exciton interaction in molecular beacons: a sensitive sensor for short range modifications of the nucleic acid structure. Nucleic Acids Res. 2001;29:E62-62.
44. Svilar D, Vens C, Sobol RW. Quantitative, real-time analysis of base excision repair activity in cell lysates utilizing lesion-specific molecular beacons. J Vis Exp. 2012. https://doi.org/10.3791/4168.
45. Horejsh D, Martini F, Poccia F, Ippolito G, Di Caro A, Capobianchi MR. A molecular beacon, bead-based assay for the detection of nucleic acids by flow cytometry. Nucleic Acids Res. 2005;33:e13. https://doi.org/10.1093/nar/gni015.
46. Krokan HE, Drabløs F, Slupphaug G. Uracil in DNA—occurrence, consequences and repair. Oncogene. 2002;21:8935–48. https://doi.org/10.1038/sj.onc.1205996.
47. Zhang H, Zhang L, Jiang J, Yu R. A highly sensitive electrochemical platform for the assay of uracil-DNA glycosylase activity combined with enzymatic amplification. Anal Sci. 2013;29:193–8. https://doi.org/10.2116/analsci.29.193.
48. Tao J, Song P, Sato Y, Nishizawa S, Teramae N, Tong A, Xiang Y. A label-free and sensitive fluorescent method for the detection of uracil-DNA glycosylase activity. Chem Commun. 2014;51:929–32. https://doi.org/10.1039/C4CC06170E.
49. Furdon PJ, Dominski Z, Kole R. RNase H cleavage of RNA hybridized to oligonucleotides containing methylphosphonate,

phosphorothioate and phosphodiester bonds. Nucleic Acids Res. 1989;17:9193–204. https://doi.org/10.1093/nar/17.22.9193.
50. Fisher TL, Terhorst T, Cao X, Wagner RW. Intracellular disposition and metabolism of fluorescently-labled unmodified and modified oligonucleotides microinjected into mammalian cells. Nucleic Acids Res. 1993;21:3857–65. https://doi.org/10.1093/nar/21.16.3857.
51. Gines G, Saint-Pierre C, Gasparutto D. On-bead fluorescent DNA nanoprobes to analyze base excision repair activities. Anal Chim Acta. 2014;812:168–75. https://doi.org/10.1016/j.aca.2013.12.038.
52. Garreau-Balandier I, Lefebvre M, Jacquard S, Caillat S, Cruz-Rodriguez L, Ishak L, Agier V, Morel F, Lachaume P, Dubessay P, Sauvaigo S, Alziari S, Vernet P. A comprehensive approach to determining BER capacities and their change with aging in Drosophila melanogaster mitochondria by oligonucleotide microarray. FEBS Lett. 2014;588:1673–9. https://doi.org/10.1016/j.febslet.2014.03.008.
53. Kreklau EL, Limp-Foster M, Liu N, Xu Y, Kelley MR, Erickson LC. A novel fluorometric oligonucleotide assay to measure O 6-methylguanine DNA methyltransferase, methylpurine DNA glycosylase, 8-oxoguanine DNA glycosylase and abasic endonuclease activities: DNA repair status in human breast carcinoma cells overexpressing methylpurine DNA glycosylase. Nucleic Acids Res. 2001;29:2558–66. https://doi.org/10.1093/nar/29.12.2558.
54. Gines G, Saint-Pierre C, Gasparutto D. A multiplex assay based on encoded microbeads conjugated to DNA NanoBeacons to monitor base excision repair activities by flow cytometry. Biosens Bioelectron. 2014;58:81–4. https://doi.org/10.1016/j.bios.2014.02.040.
55. Bennett SE, Mosbaugh DW. Characterization of the Escherichia coli uracil-DNA glycosylase.inhibitor protein complex. J Biol Chem. 1992;267:22512–21. https://doi.org/10.1016/S0021-9258(18)41702-4.
56. Jet T, Gines G, Rondelez Y, Taly V. Advances in multiplexed techniques for the detection and quantification of microRNAs. Chem Soc Rev. 2021;50:4141–61. https://doi.org/10.1039/D0CS00609B.
57. Du Y-C, Jiang H-X, Huo Y-F, Han G-M, Kong D-M. Optimization of strand displacement amplification-sensitized G-quadruplex DNAzyme-based sensing system and its application in activity detection of uracil-DNA glycosylase. Biosens Bioelectron. 2016;77:971–7. https://doi.org/10.1016/j.bios.2015.10.080.
58. Liu H, Lou Y, Zhou F, Zhu H, Abdel-Halim ES, Zhu J-J. An amplified electrochemical strategy using DNA-QDs dendrimer superstructure for the detection of thymine DNA glycosylase activity. Biosens Bioelectron. 2015;71:249–55. https://doi.org/10.1016/j.bios.2015.04.048.
59. Wang L, Lu Y, Zhang C. Construction of a self-directed replication system for label-free and real-time sensing of repair glycosylases with zero background. Chem Sci. 2020;11:587–95. https://doi.org/10.1039/C9SC04738G.
60. Zhang XF, Li N, Ling Y, Li NB, Luo HQ. Sensitive detection of active uracil-DNA glycosylase via an exonuclease III-assisted cascade multi-amplification fluorescence DNA machine. Sens Actuators, B Chem. 2018;271:9–14. https://doi.org/10.1016/j.snb.2018.05.092.
61. Chen X, Wu Y, Cao G, Wang X, Ji Z, Huo D, Xu F, Hou C. A methodology for ultrasensitive detection of sequence-specific DNA or uracil-DNA glycosylase activity. ACS Sens. 2020;5:1615–23. https://doi.org/10.1021/acssensors.0c00081.

Guillaume Gines is CNRS researcher at ESPCI Paris. He holds a PhD in chemistry-biology from the University of Grenoble. His research interests revolve around DNA nanotechnologies, biosensing, and microfluidics.

Charlotte Brusa obtained her Master's degree in chemistry at the University of Grenoble Alpes. She holds a PhD in biochemistry from Champagne-Ardenne University in 2015. She is currently a quality engineer.

Christine Saint-Pierre is a research engineer at CEA Grenoble. She obtained her degree in chemistry at the University of Grenoble Alpes, France. She developed her skills in biomolecular and analytical chemistry which allowed her to obtain the rank of research engineer. Her research interests focus on DNA modification and repair.

Didier Gasparutto is a research director at CEA Grenoble. He received his Master of Science degree in biochemistry from the University of Montpellier, France, and his PhD and his habilitation in biomolecular chemistry from the University of Grenoble Alpes, France. His main research interests include chemical and biochemical engineering of nucleic acids to study alteration and repair processes, as well as on nucleic acid-based biosensors and nanotechnologies.